Calorimetry

Executive Summary

Using a series of commercially purchased differential calorimeters to quantitatively measure the amount of energy released or absorbed within an isolated Pd-based system, we have not observed any observable quantities of heat that can be attributed to anomalous heat events (AHE) or low energy nuclear reactions (LENRs). Calorimetry is one of the few experimental campaigns carried out in our AHE search that is directly measuring heat flow from an isolated system. Methods used were focused on bulk AHE detection and not in very low mass/thin film type geometries since our calorimeters require substantial heat activity to detect AHE and we need this effect to be substantial for it to be useful and applicable to real world clean energy technologies.

A multitude of sample geometries, temperature regimes, thermal stimulations, and loading pathways were employed inside our calorimeters in efforts to induce and capture AHE. Pd nanoparticles to bulk foils were loaded in environments where deuterium pressures reached 150 ksi at temperatures ranging from -150 °C to 200 °C. Loadings up to unity were achieved, and the calorimeter system was monitored in an equilibrium state between 3-14 days for each experiment. Time sensitivity was based off thermal time constants of each calorimeter which ranged from 3-14 min; however, 5mW pulsed power as short as 100 ms could be detected. We used a variety of differential calorimeters manufactured by the Setaram company; differing in characteristics such as temperature range, available sample dimensions, and sensitivity. Overall sensitivity for each calorimeter type can be found in the table below, but in general each calorimeter required hundreds of billions of AHE events to occur over a few minutes to be observable through calorimetry. This level of activity translates to having >1 AHE event for every 100 million loaded lattice sites to be detected by our calorimeters.

Table 1- AHE Sensitivity

Calorimeter	Sensitivity	Fractional site sensitivity
MS80	50 µW	1 in 10^{11} sites
BT215	200 µW	1 in 10^{10} sites
C600	2 mW	1 in 10^{9} sites

Background

Calorimetry is the main experimental method to obtain thermodynamic data in an isolated, well controlled, and defined environment. The basic concept in calorimetry is to measure, quantifiably, how much energy/mass is inserted and/or removed from a system. The system, with one channel, is what is being monitored and anything that crosses the system boundary to the surroundings is considered an input or output from the system. In the calorimeters we used, a sensor called a thermopile[58] is attached to the outside of the channel while remaining within the system boundaries, and this is what measures which direction and to what magnitude heat is transferring around the channel.

The specific type of calorimetry employed for this project is called differential calorimetry which adds an additional control system to improve the sensitivity and resolution of our calorimeters. Instead of having only one channel inside the calorimeter there are two. They are identical channels in mass, location from calorimeter center, materials, and environmental inputs. In most of our experiments the control channel has protium gas or light water instead of deuterium or heavy water. This control will undergo the same loading ramps and be introduced to identical peak pressure conditions but we do not expect 24 MeV AHE production to form. Therefore, since the sample material, pressure environment, and temperature are the same between the 2 channels, we can subtract out the control thermopile signal from the thermopile attached to the active channel, taking a differential. This method removes many classical reactions that emit or absorb heat during Pd loading including: gas compression and enthalpy of loading summed up in Equation 1. With these more classical phenomena accounted for in the differential signal, ideally, the only signal that would be added to produce excess heat in the PdD channel is AHE. In a control test the delta between the channels would be zero in a fully closed system. The excess heat would be the measured power over a given time period. The general method of accounting for input energy in a system is the coefficient of performance energy (COP_{energy}) (Equation 2). If the COP or efficiency of the system is significantly above 1 it would indicate one of the following: energy accounting is erroneous causing false positive, classical reaction is occurring, or AHE.

$$Eqn\ 1 \quad \Delta E_{in} = \left[m_{control} \int c_{v_{PdH}} dT + \Delta H_{loading}\right] - \left[m_{active} \int c_{v_{PdD}} dT + \Delta H_{loading}\right]$$

$$Eqn\ 2 \quad COP_{energy} = \frac{E_{measd}}{E_{in}} > 1\ ,\ if\ E_{measd} > E_{in}$$

[58] Thermopile: a circuit consisting of a series of thermocouples, used for measuring minute changes in temperature (indicated as a voltage) or for generating thermoelectric current. In this case the unit is μV.

Background : Passive Calorimetry

No additional energy was introduced into the system outside of (1) loading enthalpy which self-heats, and (2) protium or deuterium isochoric gas compression (above 20 ksi up to 150 ksi) during experimental set-up prior to sample/calorimeter isolation for the remainder of the experiment. The absence of externally supplied stimulation energy makes these our most sensitive calorimetric AHE experiments. Controlling energy and mass input points and closing them off during the stable phase of an experiment makes this a closed-type calorimeter. Gas was applied using ultrapressure downtubes in each calorimeter channel. To minimize any thermal gradients up these downtubes, and thereby minimize heat flow that was not being captured radially around the channel's thermopile, a heater collar [59]was clamped to the top of each down tube using a PID loop to maintain the same set temperature at the top of the downtube as the internal calorimeter (Figure 1). Once the system is isolated there is no pathway for mass to escape. Ideally, any energy transfer would have to occur through conduction radially outward from the vessel wall into the surrounding thermopile sensor.

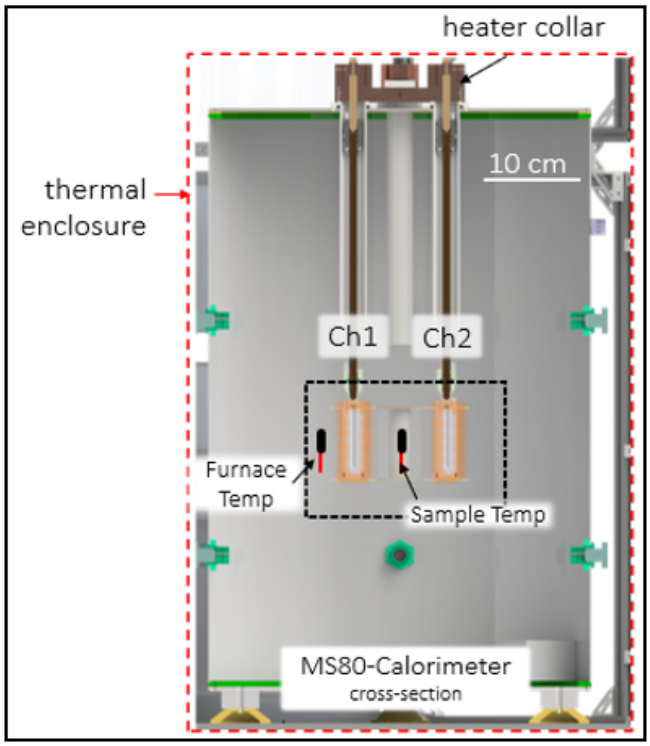

Figure 1: Heater collar location in experimental set-up.

The motivation for running these closed-type calorimetry experiments is to maximize our AHE signal sensitivity by not introducing additional noise to the system such as mass loss, electrical heaters, convection currents, etc. Removing these signals reduces uncertainty in our heat flow measurement as well, and since AHE should only be occurring in the PdD channel we should see a clear divergence in heat flow potential indicating the PdD is heating up.

Without any additional forms of stimulation, however, we are implicitly demanding that AHE occurs through loading Pd with deuterium alone. We are asking: do the kinetics of Pd loading alone cause an AHE run away reaction to a high enough intensity or flux for the thermopile

[59] Heater Collar: Bulk copper heater clamped at the top of the calorimeter and channel downtubes and maintained at the same set temperature as the calorimeter.

to measure a detectable amount of released heat from the PdD lattice? Does a loaded Pd lattice in isolation form local AHE spontaneously?

Background : Active/Stimulated Calorimetry

The active calorimetry conducted in these studies mainly focuses around adding additional electronics that were internal to each sample channel and therefore contributed to an input power over time that must be accounted for in our heat flow analysis for AHE when calculating COP_{energy}. All stimulation in gas calorimetry tests was focused on thermal stimulation either through Joule heating of the Pd sample itself or through conduction and convection heat transfer paths between a heater wire and the Pd sample. These experiments are mainly asking the question, do loading gradients caused through temperature gradients in the Pd cause deuteron hopping to a large enough extent to where we increase the probability of 2 deuterons meeting and fusing in an interstitial site?

Using active calorimetry, as opposed to passive calorimetry, involves a tradeoff; does the advantage of stimulation in helping/allowing AHE offset the lower achievable sensitivity? Fortunately, of course, this is not an either/or proposition; we were able to perform both types of experiments.

Background : Setaram Calorimeter Suite

The differential calorimeters used throughout this project were sourced from Setaram Inc. The company has extensive knowledge of the design and production of these calorimeters and is world class in terms of quality, resolution, sensitivity, and reproducibility in both academic and industrial research settings. Sourcing all calorimeters from this reputable supplier made sense in both time savings and data quality, instead of designing and troubleshooting our own custom differential calorimeters from scratch. It also, of course, will aid any other researchers interested in replicating our experiments; they will face no need to attempt to resurrect (or trust) a custom, home-built calorimeter, Four main calorimeters were used throughout the duration of the project, a basic overview of each calorimeter's specifications can be found in Table 2.

MS80 – The largest calorimeter by size containing 4 sample channels, each 35 mm in diameter, this calorimeter allowed for larger mass samples (up to 15 g) in each channel (Figure 2). Channels 1 and 2 are a differential pair while channels 3 and 4 were a second pair within the same calorimeter. The second pair would allow a second experiment to run in parallel or run as another control pair to account for any environmental changes to the system over the course of the experiment. The MS80 is the most sensitive out of all the calorimeters employed but most limited in set temperature range of 25-200 °C. It is also the least sensitive in time with a thermal time

constant [60]of 12 min. The largest heat flux range that could be reliably measured was between +/- 500 mW between channels. If heat flow from one channel to another exceeds 500 mW in this differential measurement the system saturates [61]the sensors, and we no longer would have an accurate heat flow signal until the heat flux between channels drops below 500 mW once more. Both gas and liquid type loading/AHE experiments were conducted inside this system.

C600 – 2 channel differential calorimeter optimized for high set temperature experiments (25-600 °C) (Figure 2: Cross sections of a) thermopile sensor, b) MS80, c) C600, d) BT215 with liquid N2 jacket around channels 2). The highest temperature explored was 200 °C before the channels were damaged due to a pressurized sample vessel catastrophically rupturing inside the calorimeter damaging the thermopile beyond repair. Though this instrument was damaged, the higher temperature parameter space was well explored through other campaigns including Thermal Ignition and NanoTI.

C80 – 2 channel differential calorimeter optimized for high set temperature experiments (25-300 °C). The unit dimensions are similar to the C600 unit with a slightly longer bore accessing the bottom of each channel where the thermopile sensitive volume is located. This unit was mainly utilized in initial low-pressure tests (<10 ksi) to confirm Pd loading, as well as replication experiments that are explained in detail in their respective sections of this overall report.

[60] Time constant (τ): time it takes for the heat flow signal to decay to e^{-1} from its peak maxima. It is related to calorimeter heat capacity and conductive path between the sample vessel and constant temp block, controlled by the calorimeter construction. Expressed as the time for the temperature at the element of a thermistor, with no load applied, to change to 63.2%, during a sudden change in temperature.

[61] Heat flow saturation: The thermopile sensor has a limit on sensitivity of the electrical circuit measured in uV, if the potential exceeds a limit of 20000 uV (converted to 500 mW) it is outside the linear range of the circuit and therefore inaccurate to heat flow measurement.

BT215 – 2 channel differential calorimeter optimized for cryogenic set temperatures down to -190 °C (Figure 2). This instrument was mainly used to run experiments both passive and stimulated while at unity loading conditions.

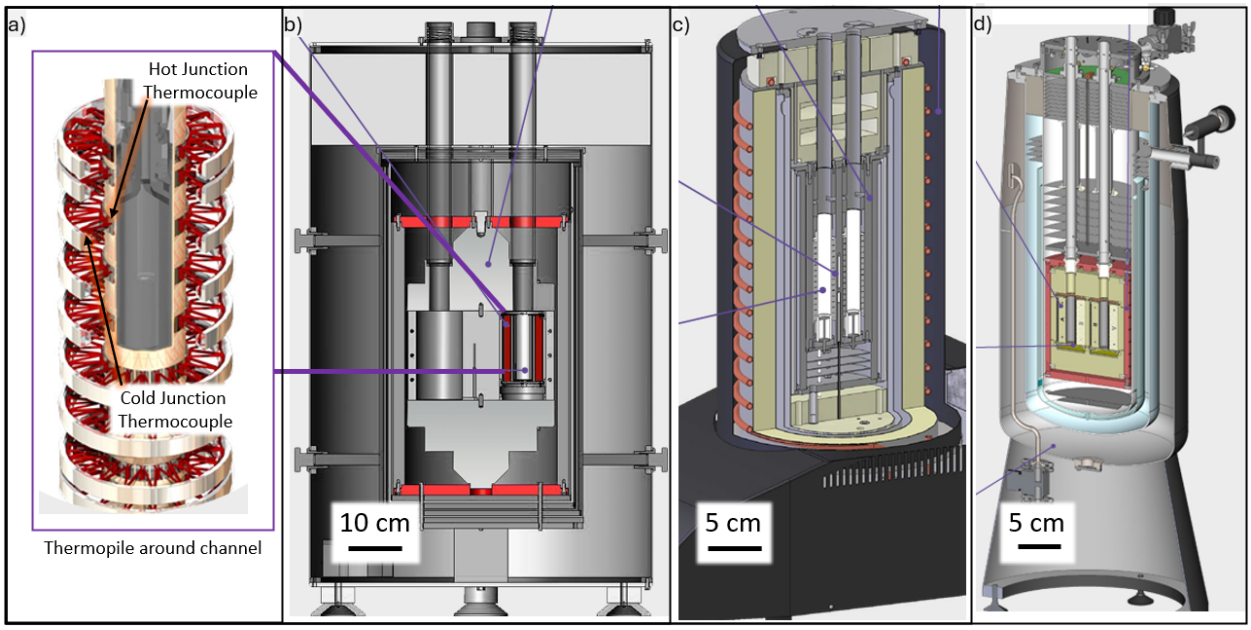

Figure 2: Cross sections of a) thermopile sensor, b) MS80, c) C600, d) BT215 with liquid N2 jacket around channels

Table 2: Calorimeter Specifications

Calorimeter Unit	Bore Diameter	Bore Length	# of Channels	Temperature Range	Sensitivity
MS80	35 mm	700 mm	4	30 - 200 °C	50 µW
C600	17 mm	350 mm	2	30-600 °C	2 mW
C80	17 mm	450 mm	2	30-300 °C	200 µW
BT215	17 mm	600 mm	2	-190-20 °C	200 µW

Methods

Methods : Samples

All samples used in calorimetry were focused on pure Pd in its various form factors that we could obtain or produce multiple grams of material. Below are the sample selection requirements we used in grading which samples were most feasible in our differential calorimeters.

- Quantity of available material to purchase should be > 5 g to allow for multiple experiments to be conducted.
- Surface area of material form factor should be maximized to reduce overall H/D loading times during experimental set up to channel isolation
- No mass should be able to escape the system throughout the duration of the experiment.
- Pd purity must be at least 99.95 at. % and ideally ≥99.99 at % pure.

The requirement for large mass negated the use of any of our very thin film geometries since the thermal mass of films is <<1 mg which would require large heat fluxes to form in a given Pd film, i.e., for >0.1 % of the Pd interstitial sites to form AHE events over a few seconds.

Foils and Wires

Pd foils of ≤250 μm were used for large sample mass experiments where we could fit >5 g into a single channel (Figure 4). High purity wires ranging from 20-250 μm in diameter were also used for some experimental runs to further increase surface area of the Pd (Figure 5). Bulk quantities of foils and wires were acquired from various material suppliers including Goodfellow, ACI Alloys, and California Fine Wire.

Nanoparticles

Significantly reducing the length scale of our Pd to where the ratio of surface area to volume was much higher was an important parameter to turn since there have been claims in LENR literature that nanoscale structures of Pd were important for loading and AHE. The size scale and geometry produced loading enhancements at the surface of the nanoparticle down to roughly 5 nm below which deterioration of absorption occurs[62,63]. Pd nanoparticles (NPs) were produced in-lab using Pd hydrogel to aerogel sublimation chemical processing. This utilized various precursor Pd salts and catalysts to induce Pd precipitation into a fine Pd nanostructure[64,65,66]. We were also able to obtain larger quantities of Pd nanoparticles with similar reaction chemistry from Goodfellow allowing us to install much larger masses >1 g of nanoparticles in each channel. The nominal diameter for nanoparticles within a chain-like structure were <20 nm in diameter with 99.99 at %

[62] Eduardo A. Crespo, Margarita Ruda, Susana Ramos de Debiaggi, Eduardo M. Bringa, Fabián U. Braschi, Graciela Bertolino, Hydrogen absorption in Pd nanoparticles of different shapes,
International Journal of Hydrogen Energy, Volume 37, Issue 19, 2012, Pages 14831-14837, ISSN 0360-3199

[63] Sachs, C, Pundt, A, Kirchheim, R, Winter, M, Reetz, M T, and Fritsch, D. "Solubility of hydrogen in single-sized palladium clusters". 2001

[64] Burpo FJ, Nagelli EA, Morris LA, McClure JP, Ryu MY, Palmer JL. A Rapid Synthesis Method for Au, Pd, and Pt Aerogels Via Direct Solution-Based Reduction. J Vis Exp. 2018 Jun 18;(136):57875. doi: 10.3791/57875. PMID: 29985323; PMCID: PMC6101767.

[65] Burpo, F., Nagelli, E., Morris, L., McClure, J., Ryu, M., & Palmer, J. (2017). Direct solution-based reduction synthesis of Au, Pd, and Pt aerogels. Journal of Materials Research, 32(22), 4153-4165. doi:10.1557/jmr.2017.412

[66] Du R, Joswig JO, Hübner R, Zhou L, Wei W, Hu Y, Eychmüller A. Freeze-Thaw-Promoted Fabrication of Clean and Hierarchically Structured Noble-Metal Aerogels for Electrocatalysis and Photoelectrocatalysis. Angew Chem Int Ed Engl. 2020 May 18;59(21):8293-8300. doi: 10.1002/anie.201916484. Epub 2020 Apr 6. PMID: 32187791; PMCID: PMC7317422.

purity claimed. 99.9% purity was verified with in-house resources including energy dispersive x-ray spectroscopy.

Methods : Sample Retention for each Campaign

Ultrapressure Vessel Design

The hardware component that made all calorimeter experiments possible at these extreme pressure conditions was the cylindrical pressure vessel. The vessel was optimized to ensure containment of hydrogen-based gases, and therefore the chosen material, Toughmet, was selected to avoid embrittlement from exposure to hydrogen. A double compression seal was designed for both the small and large bore vessel types. The smaller vessels used a "football" type Toughmet insert that sealed against both the vessel inlet and a BeCu downtube that provided gas access all the way down the calorimeter bore length (Figure 3a). Once at ultrapressure conditions each channel used ultrapressure valves at the top of each channel on the outside of the calorimeter to isolate the channel from the larger pressure source to ensure that energy and mass transfer is minimized along that pathway. The larger pressure vessel used what was called internally as, a UFO seal, sealing the vessel cap to the main vessel body. The vessel cap then used a similar sealing methodology as smaller vessels to connect to the BeCu downtube gas inlet (Figure 3b). For both sets of hardware all sealing surfaces were captured in a leak detection system that would alert the user that a given sealing surface was leaking. This is crucial because a small leak is manifested in the calorimeter

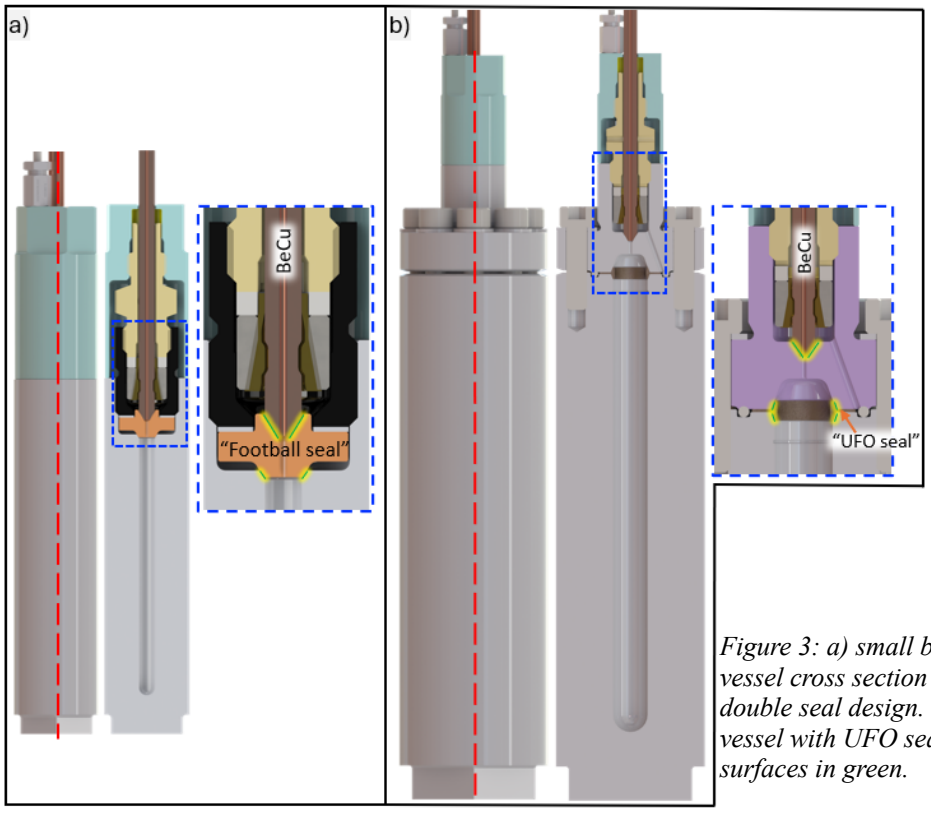

Figure 3: a) small bore pressure vessel cross section showing double seal design. b) large bore vessel with UFO seal. Sealing surfaces in green.

as heat flow, and so the auxiliary leak detection system was able to quickly confirm or deny if a transient heat flow signal was pressure based. All channels were monitored by ultrapressure transducers during the entire course of the experiment.

Passive Foil/Wire

The foils and wires were held loosely within a thick-walled pressure vessel that was then inserted into each channel of the calorimeter. Foils were rolled up tightly with a gold mesh sheet separating foil surfaces from one another to allow gas access and not slow down protium/deuterium loading kinetics at each surface (Figure 4). In other experiments, microwires of 20 μm diameter were bundled together in packs of 2000 to maximize the mass that could be placed inside a pressure vessel (Figure 5).

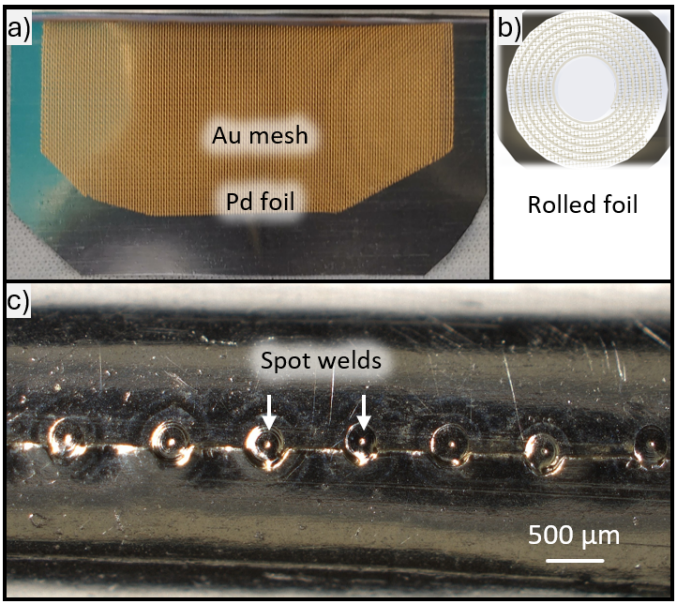

Figure 4: a) Rolling process with mesh interlayer, b) axial view of rolled sample, c) spot welds of foil seem to prevent unraveling.

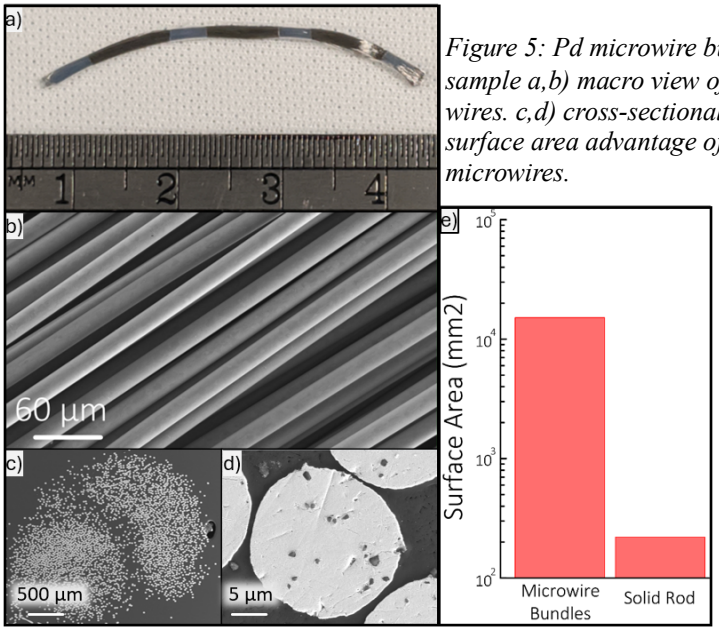

Figure 5: Pd microwire bundle sample a,b) macro view of 20 µm wires. c,d) cross-sectional views. e) surface area advantage of microwires.

Passive Nanoparticles retention

Due to nanoparticles being inherently small, they are prone to becoming airborne which can be dangerous for users in proximity to the experiment and could easily contaminate many instruments, including the calorimeter, increasing uncertainty in future experiments. We are also inserting nanoparticles into a high-pressure environment, that could leak catastrophically, worsening this contamination and health issue. The retention designed for passively monitoring nanoparticles in our MS80 calorimeter can be seen in Figure 6. This stainless-steel tube was

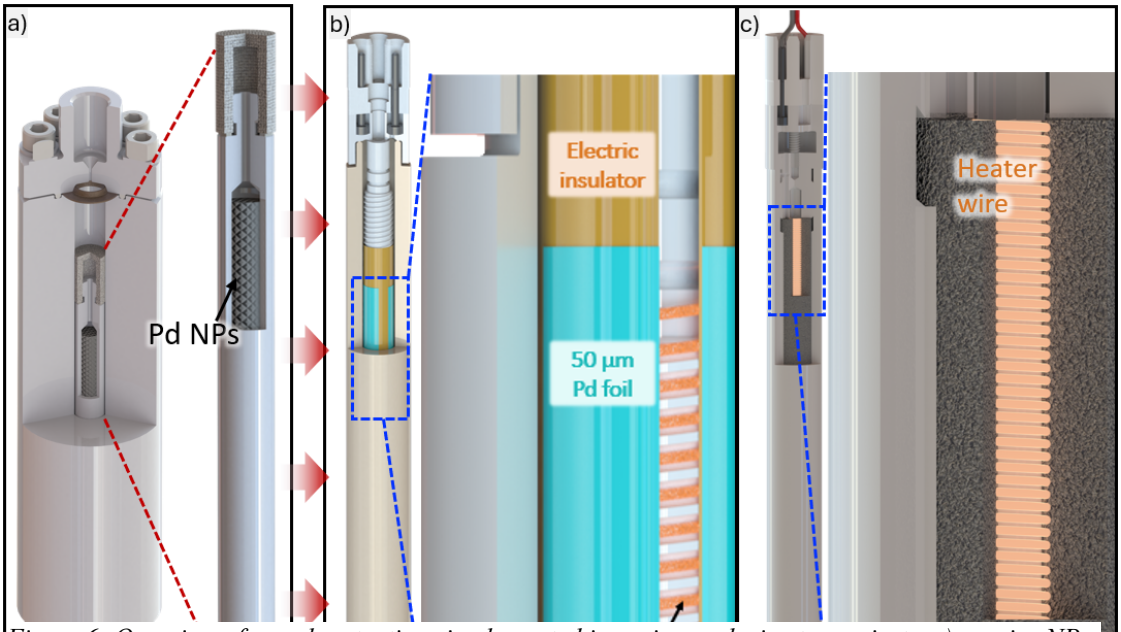

Figure 6: Overview of sample retentions implemented in various calorimeter projects. a) passive NP. b) foil/wire stimulation. c) NP stimulation.

closed on one end with a compression seal and had a porous stainless steel gas filter threaded on the other. The average pore size of this filter was 0.5 µm with a 1 mm thick cross-section making escapement of particles through the filter difficult without becoming entrapped. Protium and deuterium flow into the retention was still possible allowing nanoparticle loading and to prevent inadvertent formation of uncontrolled pressurized volume within the vessel. This minimizes risk for personnel when handling material and any damage to instruments near or internal to the calorimeter.

Stimulated Foils/Nanoparticles

Thermally stimulating foils and NPs required the same type of heater wire composed of 150 µm diameter NiCr80. For the foil retention, bare NiCr wire was spooled onto a 2-start ACME thread design to maximize the length of wire used and ensure wires entered and exited the retention on both sides of the vessel (Figure 6). Kapton film (25 µm thick) or bare fiberglass fibers were inserted in between the Pd foil and the heater wire to prevent shorting.

Fiberglass insulated NiCr wire was used in the NP retention to maximize surface contact of the NPs to the heater spool in the center (Figure 6c). Similar to the passive NP retention, only one end of the retention was open to gas and also contained a porous titanium sheet with pore size of 1 µm to minimize NP escapement throughout the duration of the experiment.

High Pressure electrochemistry

High pressure electrochemical loading inside the differential calorimeter required improvements to electrical access to each pressure vessel. To account for all energy inputs going into the vessel for each channel a total of eight isolated Pt wires were used in ultrapressure electrical feedthroughs. These feedthroughs are identical in design concept to epoxy feedthroughs discussed in the hardware section of this report, with the additional constraint of sealing around a 5/16” inner diameter instead of a ½” or ¼” diameter used in later iterations of 500 ksi HPE experiments that

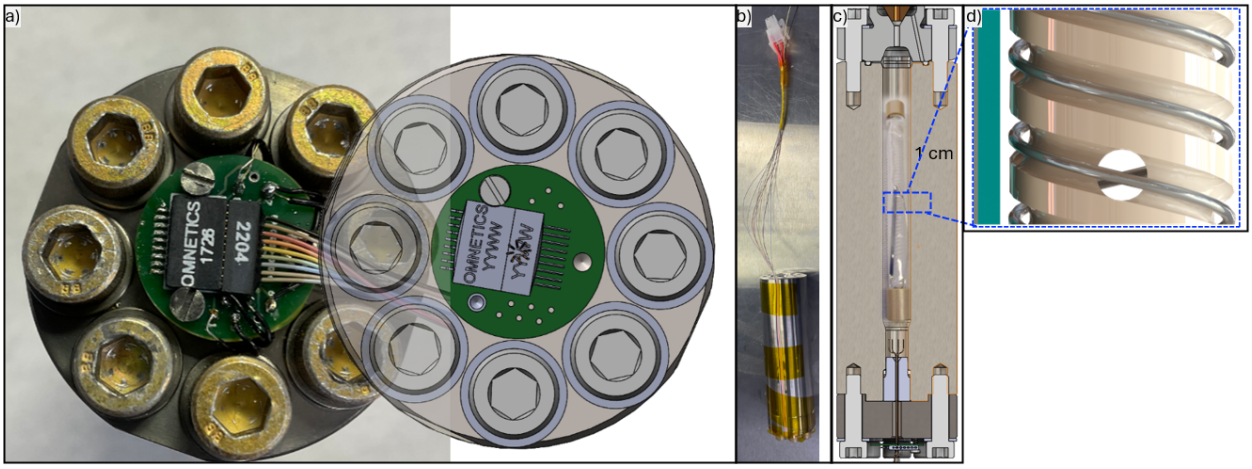

Figure 7: a) Looking at the bottom of the HPE calorimeter vessel with custom PCB connector and wires that were fed along a track on the side of the vessel. b) Overview image of wires fed along outside of vessel. c) vessel cross section with detail d) showing retention of electrodes (Pd is the foil, Pt the spiral wire).

were not carried out in a closed calorimeter enironment. These feedthroughs carried the constant current voltage across the Pd cathode and the Pt anode, *in-situ* 4-wire RTD in contact with electrolyte, *in-situ* 4-wire resistance Pd circuit for H/D loading montoring, and voltmeter circuit. All circuits were terminated at the bottom of the vessel as seen in Figure 7 where a custom PCB connector was used to maintain low profile and maximize vessel wall contact with calorimeter channel wall. The entire wired vessel assembly is seen in Figure 7b,c. A teflon mesh was placed between the Pd and Pt electrodes to ensure there were no short circuits during the experiment.

Results

Results : Passive calorimetry : At 50ºC to 150°C

Experiments completed where we kept the pressure and temperature constant, once the calorimeter was pressurized, were split up according to sample form factor and set temperature. Experiments completed successfully always maintained a 100 ksi or 150 ksi gas pressure internal to each channel. Table 3 summarizes the various experimental conditions we conducted on Pd samples with each experiment, on average, remaining in an isolated, stable state for ≥4 days. All tests were completed with a protium control in 1 of the 2 channels.

Table 3: Passive Calorimetry Parameter Space

		Temperature (°C)					
		-100	-50	50	100	150	200*
Pd Form factor	Foil						
	Wire						
	3µm powder						
	NPs (15 nm)						

* No other samples were tested at 200 °C due to damage of the high temperature calorimeter (C600)

Interpretation of the data focused on any excess-heat measurements that would then need to be thoroughly examined through instrument, calibration, user error, or classical explanations, before postulating an AHE explanation. The data interpretation relies heavily on establishing a 'baseline', with deviations from this baseline indicating that one channel of the calorimeter is hotter or colder than the other. The detection resolution of the experiments is determined by the magnitude of these baseline fluctuations. The resolution for most passive experiments was defined by upper and lower limits defined by +/- 2σ from the baseline average. For heat flow data reported in this section the

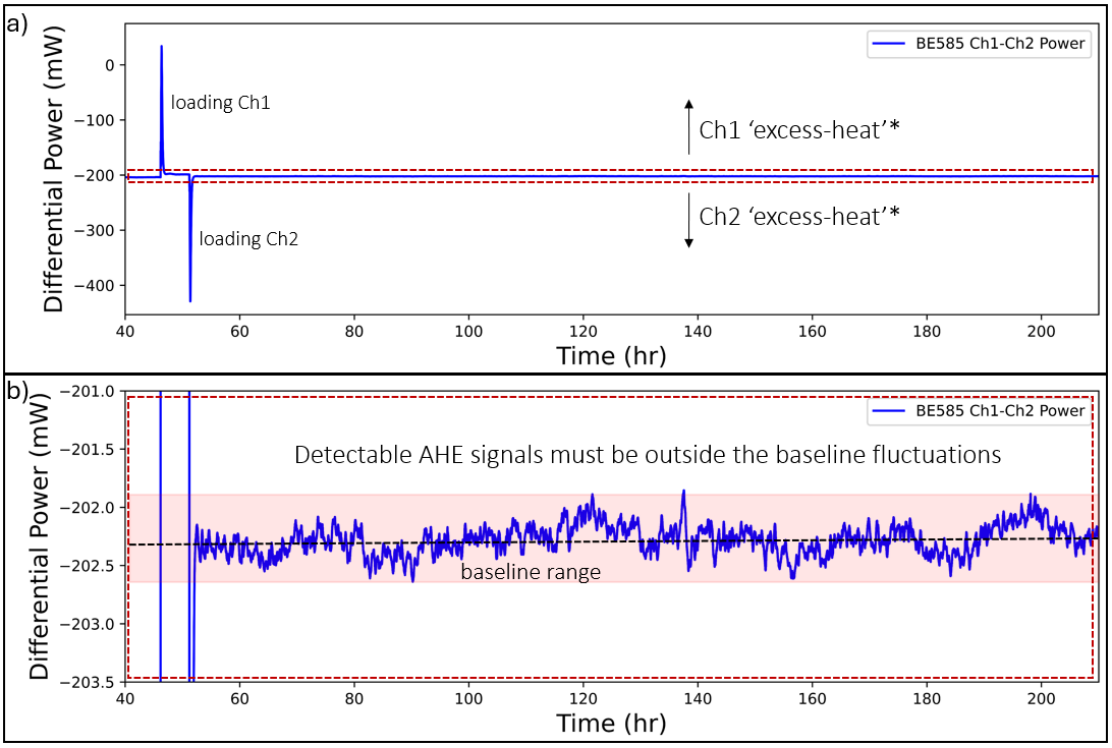

Figure 8: a) Overview of calorimeter heat flow in a typical experiment. Loading itself produces heat flow from H/D loading into the Pd lattice and is ignored for analysis. b) Heat flow axis is expanded to only the baseline range where the calorimeter stabilized after gas isolation. No abnormal signals detected.

units are in mW (converted from thermopile raw signal collected in μV).

Most experiments did not show anomalous behavior beyond the baseline fluctuations and therefore did not warrant further analysis and investigation of spurious heat flow signals. For calorimeter experiments using foils and wires between 50 and 100 °C the heat flow data was extremely stable (Figure 8). Fluctuations within baseline are small temperature gradients across the large calorimeter thermal mass which are <0.25 °C and occur over 24-hour timescales, much longer than any short-term releases of heat within a given channel. Anomalous signals observed throughout all passive calorimetry fell within the categories listed in Table 4.

Table 4: False Signal Sources in Passive Calorimetry

Cause of False signal	Resulting Heat Flow Profile	Controls
Pressure loss (<1000 psi) in 1 or more channels	Gradual but consistent diversion from heat flow baseline, 'cooling' the channel that is leaking through mass loss	• Monitored by pressure transducers
Catastrophic pressure loss (>1000 psi)	Sharp diversion from heat flow baseline, 'cooling' the channel that is leaking through convection and mass loss	• Monitored by pressure transducers • Internal channel RTDs
Heater collar failure	Baseline shift over 3-4 hours then stabilizing	• >4 RTD probes on heater collar looking for temperature gradients across the collar
Calorimeter enclosure heater failure	Baseline range 2-5x larger and fluctuates cyclically over 24 hour period	• >4 RTD probes at various locations on cart external to calorimeter
Calorimeter heater power shifts	Baseline shift over 3-10 hours then stabilizing	• Recording input power levels from calorimeter heater with Setaram software
Liquid nitrogen source is empty	Heat flow drifts uncontrollably until stabilizes with room temperature	• Liquid nitrogen reservoir liquid level probe • RTDs in reservoir • Facility tank fill % recorded every minute

Prior to operating matured calorimetry experiments that maintained exceedingly good thermal stability and isolation from external variables outside the calorimeter system, one experiment produced a heat flow signal indicating the PdD was releasing heat. This test was conducted at 100 ksi deuterium and at 50 °C with no other thermal stimulation, a completely passive test. The differential heat flow is plotted in Figure 9Figure 9: a) Heat flow data showing numerous spikes in the direction that indicates PdD emitting energy (baseline noise subtracted). b) Spread in peak power amplitude reached for a given heat flow spike, not all peaks are of same magnitude. The spikes in heat flow were sporadic throughout the duration of the test, not occurring at specific times of the day or in line with variations in pressure change or external RTD variation (see Appendix for further data streams).

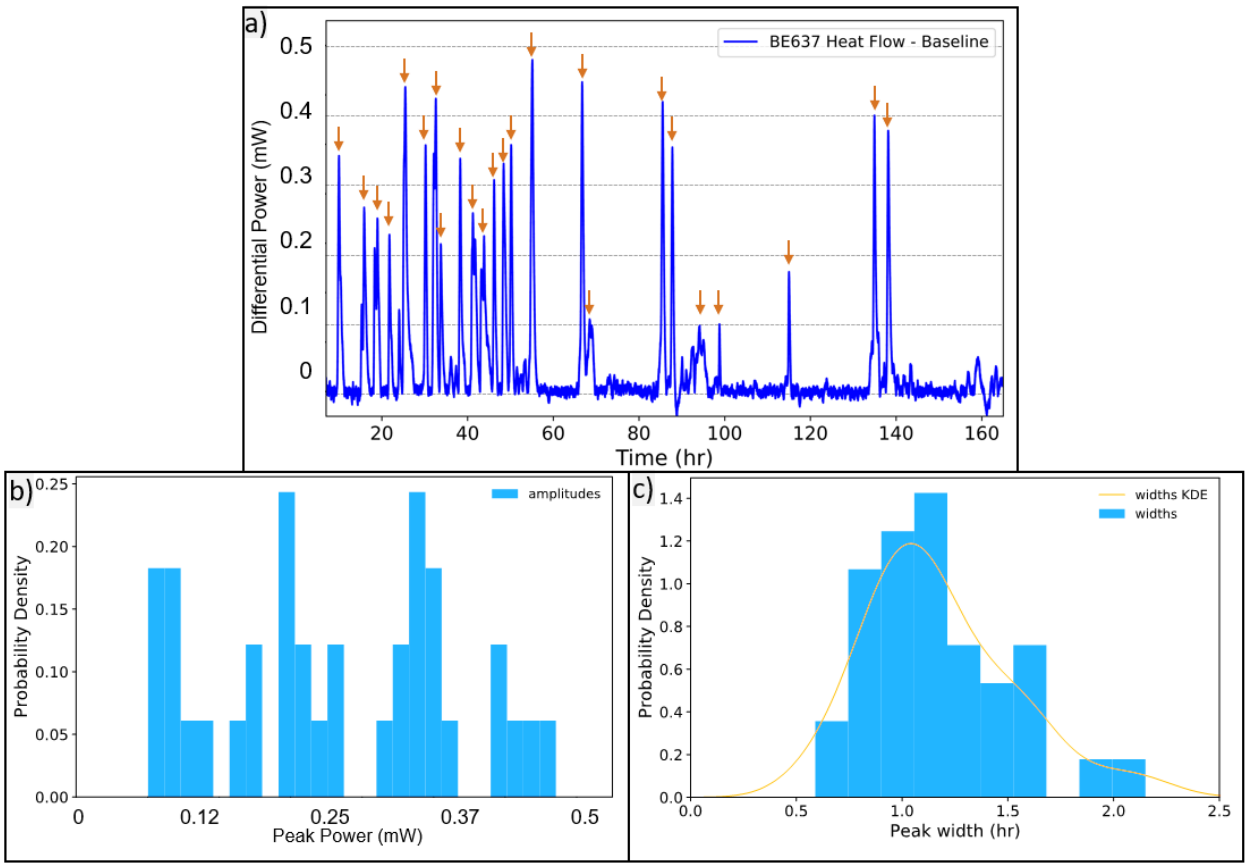

Figure 9: a) Heat flow data showing numerous spikes in the direction that indicates PdD emitting energy (baseline noise subtracted). b) Spread in peak power amplitude reached for a given heat flow spike, not all peaks are of same magnitude. c) Spread in how long the peak forms and decays over time showing that there is variable duration of power for each event.

This signal never formed again within any of our calorimeter systems including the same MS80 that this data was collected.

At the time this signal was observed we did not have a fully enclosed thermal enclosure or minor forms of vibration dampening to the calorimeter which could lead to extraneous influence on the heat flow data that was not detected by auxiliary sensors. Extensive post characterization on the Pd sample was completed, with no abnormal surface morphologies or compositional variation measured compared to the source material. We did find evidence that minor movements of the channel downtube would produce large transient behavior over short time scales of 10-30 min in thermopile voltage signal, but we could never definitively locate the source of this heat flow signal. And after iterating and reproducing upwards of dozens of these passive calorimetry experiments with stable heat flow results, we concluded this signal was not relevant to observing AHE or characterizing its behavior because it could not be replicated. Further examples of other false signals can be found on Synergy under the Calorimetry Project.

Results : Passive calorimetry : At -150ºC to -50°C

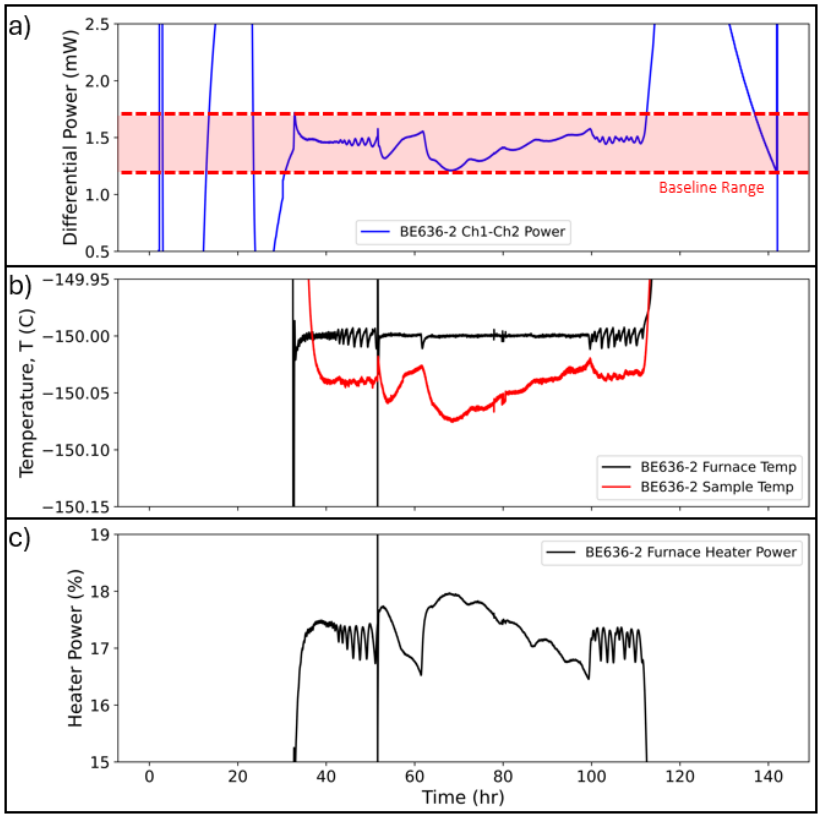

Figure 10:a) Heat flow axis showing small fluctuations over 140 hours related to calorimeter heater and LN2 cooling instabilities. b) RTDs of samples and furnace (heater) to maintain -150 °C. c) Power input from BT215 converted to % of total constant current DC power.

Performing differential calorimetry at these temperature regimes in both bulk and NP forms helped ensure we were maximizing our loading in the Pd lattice, and (because of very low surface kinetics and deuterium diffusion) locked in the Pd loading once isolated and stabilized at these temperatures[67]. The Pd was loaded at room temperature and 150 ksi protium/deuterium prior to cooling down to final set temperature to ensure the kinetics timescales of the loading process would not exponentially decrease and hence not fully load when <-50 °C. Figure 10 shows a typical heat flow result from a cryogenic calorimetry run at -150 °C where we see no significant deviations from the baseline readout between the control channel and the active PdD channel. The short-term deviations over 10-20 min timescales are from the BT215 heater fluctuation power to maintain -150 °C, and was confirmed by noting that the heater power changed 20-30 seconds before we start to see the heat flow response clearly indicating this heat flow change is not caused by internal channel sample reactions. In Appendix Figure 19, another calorimeter experiment is shown where we kept baseline fluctuations to <0.2 mW and still observed no unexplained anomalies in the readout. NPs in passive experiments showed similar results to foils and wires. Images and additional details on NPs based experiments can be found in the Appendix.

Results : Passive calorimetry : At 200°C

When elevating the set temperature, the equilibrium loading process results in a reduced peak loading of the Pd lattice; however, the deuterons will have a higher average kinetic energy for

[67] F. Scaramuzzi, Gas loading of deuterium in palladium at low temperature, Journal of Alloys and Compounds, Volume 385, Issues 1–2, 2004, Pages 19-27, ISSN 0925-8388.

interstitial site hopping, testing the hypothesis that increased lattice site hopping increases probability for 2 deuterons to meet and fuse at a single site. The highest temperature that we could achieve while at 100 ksi and inside a closed calorimeter was 200 °C inside the C600 unit. Out of the 2-3 tests in which we collected data at 150-200 °C we did not observe any unexplained heat flow fluctuations in our data. Unfortunately, we could not run further tests at these levels safely because we found that the pressure vessel material, holding the sample and gas inside the calorimeter channel, fails catastrophically from high temperature embrittlement of the Toughmet material at elevated temperatures (Figure 11). Through repeat vessel failure experiments, external to a calorimeter, we found these failures occur regardless of gas type, i.e., also occurred in He. Since this failure effectively can bisect a vessel and form projectiles, we discontinued our efforts in probing high temperature holds over long time periods with these vessels.

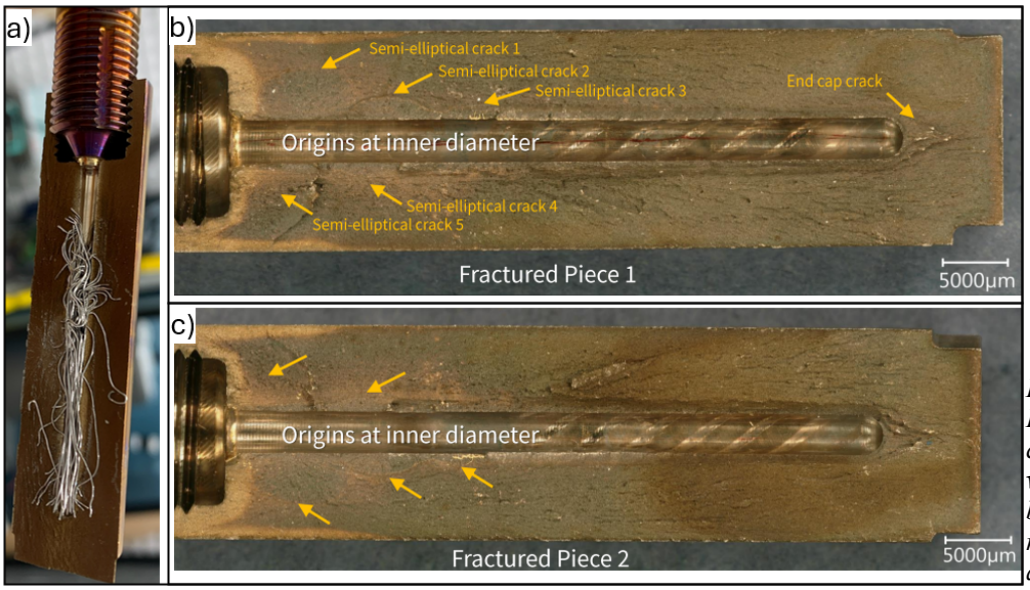

Figure 11: a) Ruptured C600 channel vessel with Pd wires inside. b) and c) both halves of a vessel rupturing axially with a brittle fracture.

Results : Stimulated calorimetry : Foils and Nanoparticles at 50ºC to 100°C

Up to this point the results we've described have only been looking at loading and set temperature as variables that could induce AHE to occur spontaneously. In this and remaining results sections we are actively adding energy to the Pd system through conduction heating means in order to attempt to knock the system out of equilibrium. Adding energy to the system over a few seconds timescale is testing if inducing loading fluxes/deloading to the sample could increase short term deuteron site hopping enough to cause D-D fusion.

For us to understand if we are producing more energy than we are putting in we are utilizing the COP_{energy} calculation discussed in the concept section, and we are adding an additional variable to the energy balance of the system seen in Equation 3. As a reminder, the heating is from a NiCr wire so the DC input power can be calculated using current (I) and voltage (V). Heating these wires in close proximity to the sample, we were able to heat our Pd samples to at least 350°C and above 450 °C at the surface of Pd in contact with wires based on COMSOL simulations (Figure 13). Equations 3 and 4 are only for stimulating a single channel in the calorimeter, so do not treat the differential signal; however, for us to heat the sample up to >350 °C we would saturate the heat flow signal to the upper or lower range of the thermopile sensor. Therefore, we performed a separate series of experiments where we applied the same input power to both channels and ideally subtract out the input power signal since it is a differential calorimeter (Equation 5 and 6). This is not an ideal system, so we had to account for about 2 % uncertainty in the COP_{energy} calculation.

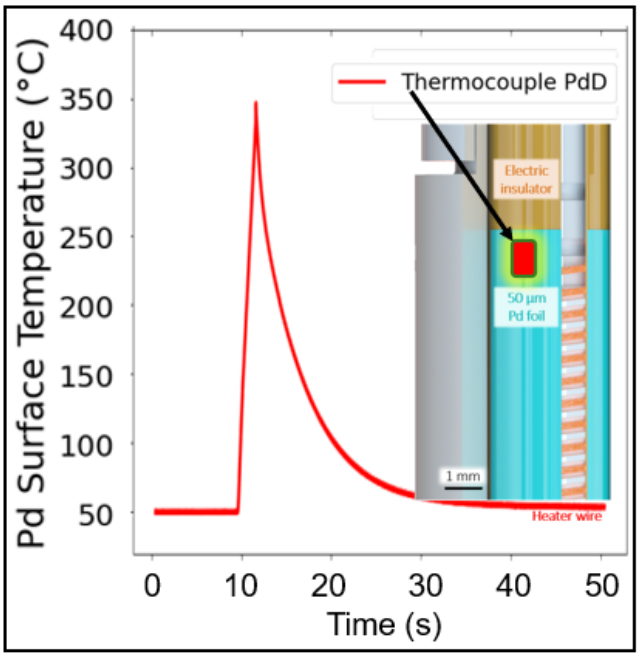

Figure 13: In-situ thermocouple readout during thermal pulse of wire heater. CAD model in insert used in COMSOL heat transfer simulation.

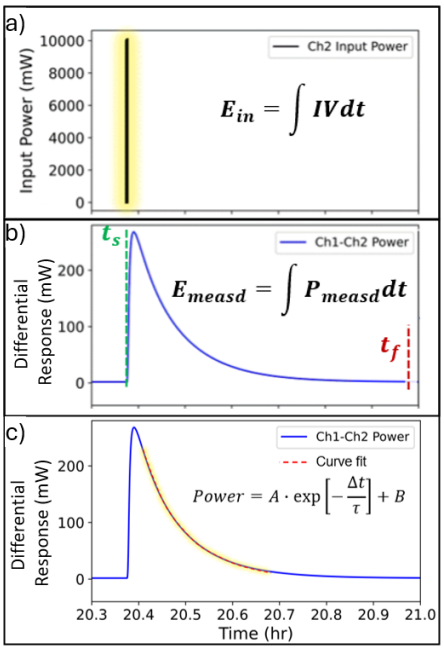

Figure 12: a) Electrical pulse sent through heater wire. b) Calorimeter heat flow response. c) Exponential decay fit of heat flow.

Eqn 3

$$\Delta E_{1ch} = \left[m_{control} \int c_{v_{PdH}} dT + \Delta H_{loading} + \int IV_{PdH} dt\right] - \left[m_{active} \int c_{v_{PdD}} dT + \Delta H_{loading}\right]$$

Eqn 4

$$E_{measd} = \int P_{measd} dt \ , \quad COP_{energy} = \frac{E_{measd}}{E_{1ch}}$$

Eqn 5

$$\Delta E_{2ch} = \left[m_{control} \int c_{v_{PdH}} dT + \Delta H_{loading} + \int IV_{PdH} dt\right] - \left[m_{active} \int c_{v_{PdD}} dT + \Delta H_{loading} + \int IV_{PdD} dt\right]$$

Eqn 6

$$COP_{energy} = \frac{E_{measd}}{E_{2ch}}$$

The experimental results presented are analyzing the result's COP_{energy} value and determining if it is significantly above the value of 1 indicating excess heat in one channel, and calculating the thermal time constant from the calorimeter response in heat flow for each thermal stimulation pulse. Changes in the thermal time constant can indicate changes to the conductive path between the differential channels in the calorimeter. Monitoring if the conductive path changes during a test is important to ensure our thermal calibrations are still applicable. Figure 14 shows the COP and time constant results for Pd Foils stimulated in one channel at a time. These results give no indication of increasing thermal time constant, and COP remains below 1, indicating we are not observing excess heat from this stimulation method while at 150 ksi. We are not able to capture

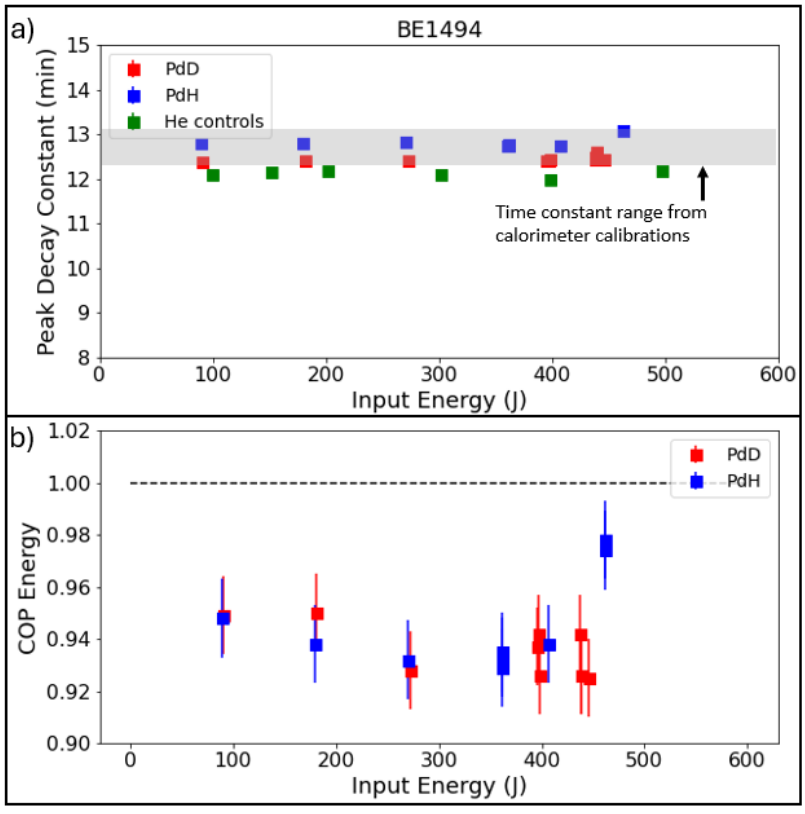

Figure 14: a) Calculated time constants from various levels of thermal stimulation energies. b) COP energy for each stimulation condition with a dashed line threshold set at 1.0.

100% of the input energy from the heater wire with the thermopiles, which is why we are below a COP of 1. One major reason for this is that we had over 6 feet of fine gauge copper leads running down the channel bores inside the calorimeter that are not within the thermopile sensor area, and therefore any minor joule heating from these wires was not captured inside the closed system.

Thermally stimulating NPs in both protium and deuterium was conducted similarly to foils with the main difference being a separate retention to safely handle and test the NPs. The results in Figure 15 show a similar story for both 3 µm Pd particles/ grains and 15 nm NPs where the time constant and COP are stable across the range of thermal input energies we used. All COPs in all experimental runs remained below 1 and the results between the PdH control and PdD were with experimental uncertainty of the measurement. No AHE signals detected.

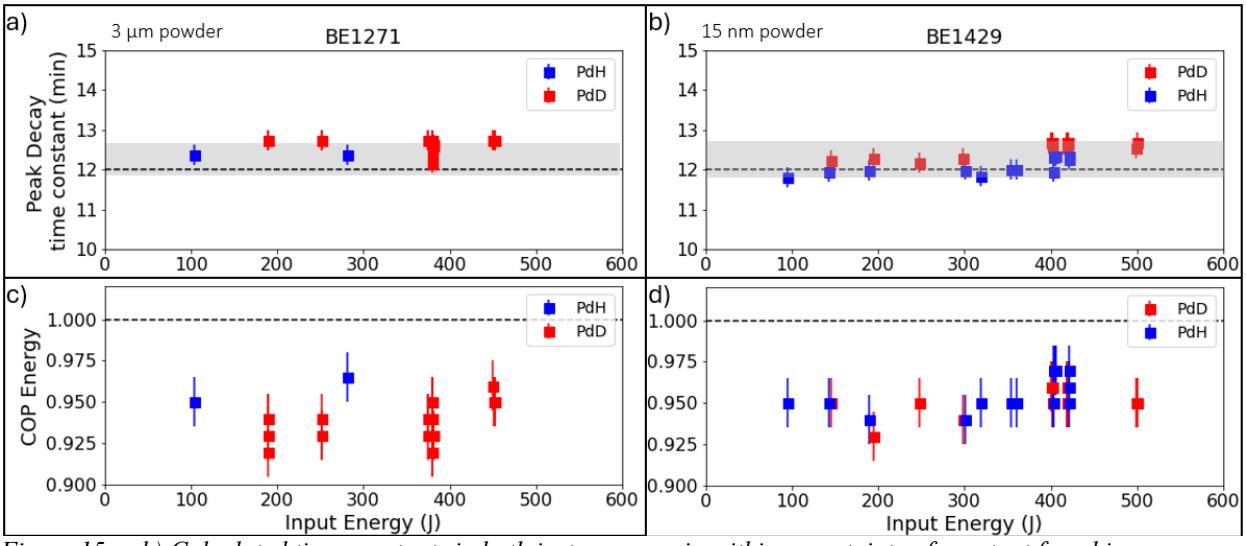

Figure 15: a,b) Calculated time constants in both isotopes remain within uncertainty of constant found in calibrations. c,d) COPs for various stim conditions, none above 1.0.

Results : Stimulated calorimetry : Wires and Nanoparticles at -100ºC to -50°C

Cryogenic campaigns with identical forms for thermal stimulation tested the same hypothesis as stated in the previous section, i.e., that loading fluxes across a sample lattice might induce D-D fusion. Below are COP results collected at -100 and -50 °C calorimeter set temperatures, points at which the initial loading condition of the Pd wire and or NPs should be at or near unity in protium and deuterium (Figure 16). Results show we did not observe excess heat at these cryogenic conditions and under these thermal impulse parameters.

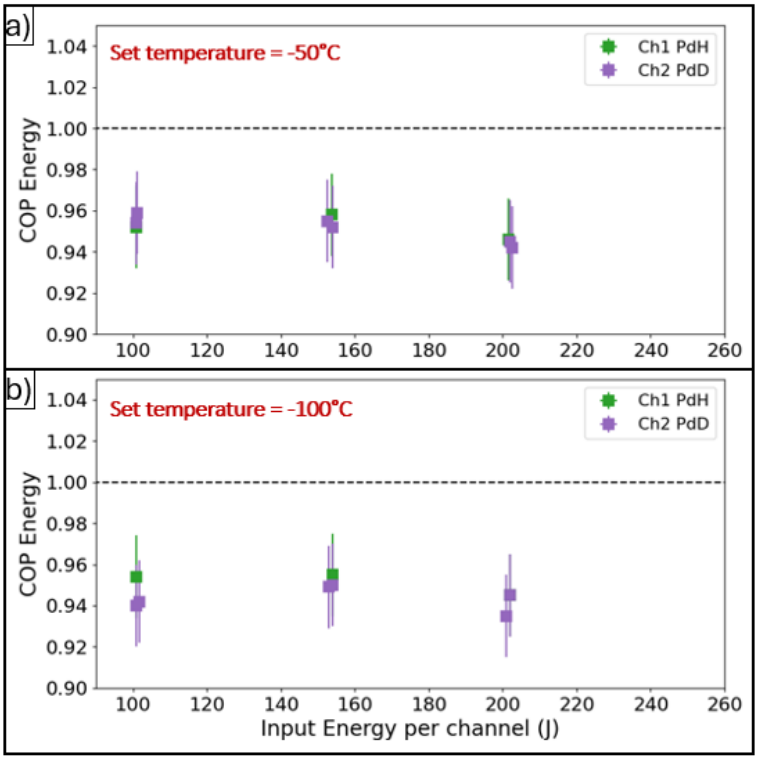

Figure 16: a,b) COP results at -50 and -100 °C set temperatures where no stimulation conditions result in a COP >1.

Results : HPE calorimetry :– At 35 to 100 °C

The materials and electrolytes used for this set of calorimeter experiments are identical to ones used in the general high pressure electrochemical experiments conducted between 150-500 ksi. For more detail on electronics used and current densities used please refer to the HPE section of this report. Both heavy and light water HPE experiments were carried out inside the MS80 calorimeter. The main salt used employed in the high purity water was LiOH/LiOD depending on which isotope was being tested in a given channel vessel. As shown in figures in the sample retention section the input power and other diagnostic read out circuits gained access to the ultrapressure liquid environment through the bottom of the vessel inside each channel of the MS80. The downtube supplied the pressure to the system utilizing a screwjack pressure system external to the thermally isolated environment around the calorimeter. For each test the calorimeter channels were first electrochemically loaded with an initial constant current set point between 5-15 mA. This was completed with full submersion of the electrodes in the electrolyte, and allowed for faster initial loading of the Pd. This section of heat flow data is not analyzed since the sample is not at pressure and the calorimeter is in a transient state making analysis in terms of measured power highly inaccurate during this time period. Once the sample reaches near the peak R/R0 value (i.e., 2.0 for PdD) the pressure ramp is started for both channels at the same time and rate. The dual channel press-up is only possible when we are using Pt as the control and are able to use a single water isotope for a given experiment. The screwjack is hooked up to each channel in parallel,

effectively tying both channel volumes together. It should be noted the heat flow loss through the path between the 2 channel downtubes is negligible since the volumes are only connected to each other by a 750 μm diameter BeCu tube of over 2 m in total length, making the conduction path exceedingly small in both cross-sectional area and overall electrolyte fluid conductance over that length scale. The only section of heat flow data analyzed was the portion after a total pressure between 150-200 ksi was reached and isolated. This pressure is typically held in this equilibrium state for 20-40 hours for a given experiment.

To avoid isotopic contamination a separate screwjack system was dedicated to a given water isotope, heavy or light water. The control sample utilized for each calorimeter had a cathode made of Pt with similar surface area, mass, and surface finish to the Pd foil used in the active channel. Making the control a Pt-Pt system allowed us to monitor heat flow formation that may occur due to small variations in Pd loading over the course of the equilibrium period of the experiment. Aside from loading and measured power, other data streams collected to account for all input power signals include: variation in lead resistance and source/sense circuits for the in-situ RTD, all of which have measurable levels of input power to the electrochemical system inside the thermopile area or are counted as power loss on the outside of the calorimeter.

A clean set of HPE calorimeter experiments can be seen in Figure 17 where one is using heavy water and the second light water. Both experiments are using close to the same current density set points with an input current of -30 mA. Accounting for all measurable sources of input power and power losses the measured power (red or blue) is slightly below the input power (green) over the majority of the experimental time window displayed. Points where we see input power drop below measured power levels translate to a COP_{power} <1.05. This COP_{power} level is below the threshold to be statistically significant and auxiliary data streams including abrupt voltage changes, pressure variation, and external RTD variation occur seconds before these increases in heat flow indicating this is a system response to small changes in equilibrium between system and surroundings. No measurable levels of excess heat at either 35 °C or as high as 100°C were observed during these experimental runs. More detail can be found on the Synergy experimental pages and Appendix for this section.

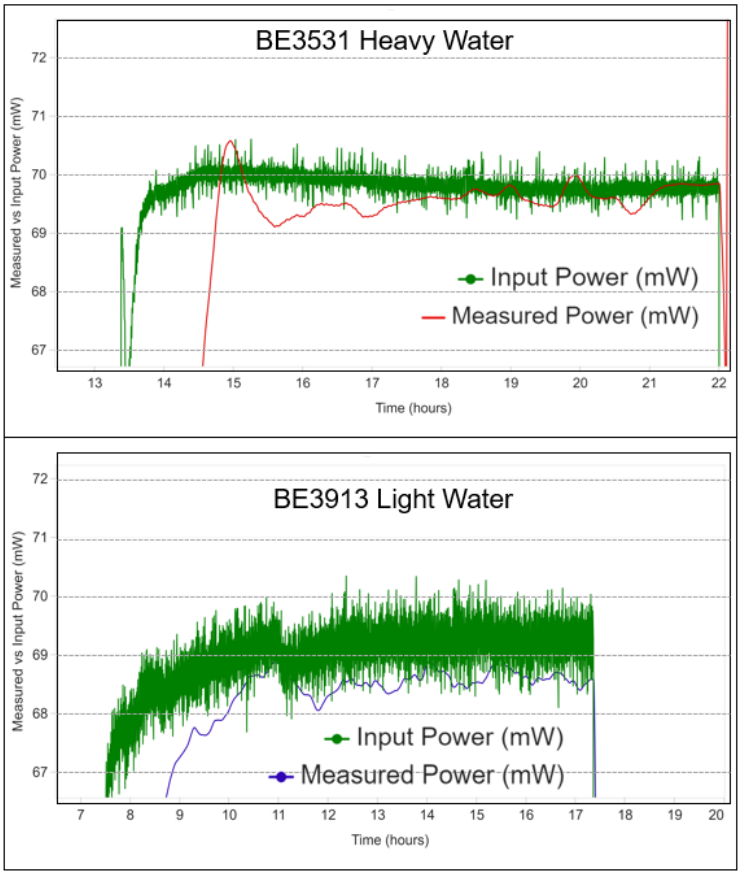

Figure 17: Light and heavy water electrochemical heat flow data overlayed with the total input power to the system. The input power remains above measured power due to the calorimeter being a real system with unaccounted for heat leaks.

During the course of operational HPE with these calorimeters we did observe heat flow signals that turned out to be false positives. These signals formed when there was an abrupt voltage change/instability, usually a drop of a few volts at constant current, where then the heat flow settled back to equilibrium after 3-4 time constants measuring power that was significantly above input power levels being supplied to the system (Figure 18). This effect was reproducible from experiment to experiment and more importantly could be replicated in light water systems. This inversion between input and measured power could also be produced just using Pt electrodes without Pd altogether making it clear this has nothing to do with lattice mediated fusion. At the time the experimental results were collected, we were still utilizing an electrolyte solution that contained heavy or light forms of methanol. This low molarity of methanol was used to stop the electrolyte from freezing at ultrapressure conditions >100 ksi while at 35 °C.

After troubleshooting possible errors in input power accounting to explain this result it was decided to increase the set temperature to 50 °C or above and remove the methanol additive altogether to remove it as a possible variable. With the methanol removed this phenomenon, increased measured power after a voltage instability, disappeared from the heat flow data in both light and heavy water experiments at ultrapressure conditions (Figure 17). The hypothesis at the time of this report is that

the methanol was possibly reducing in some fashion, forming a side exothermic reaction that was only occurring in the electrolyte. This would be a more classic chemical reaction that was reaching its own equilibrium reaction rate explaining the sustained increase in measured power over time.

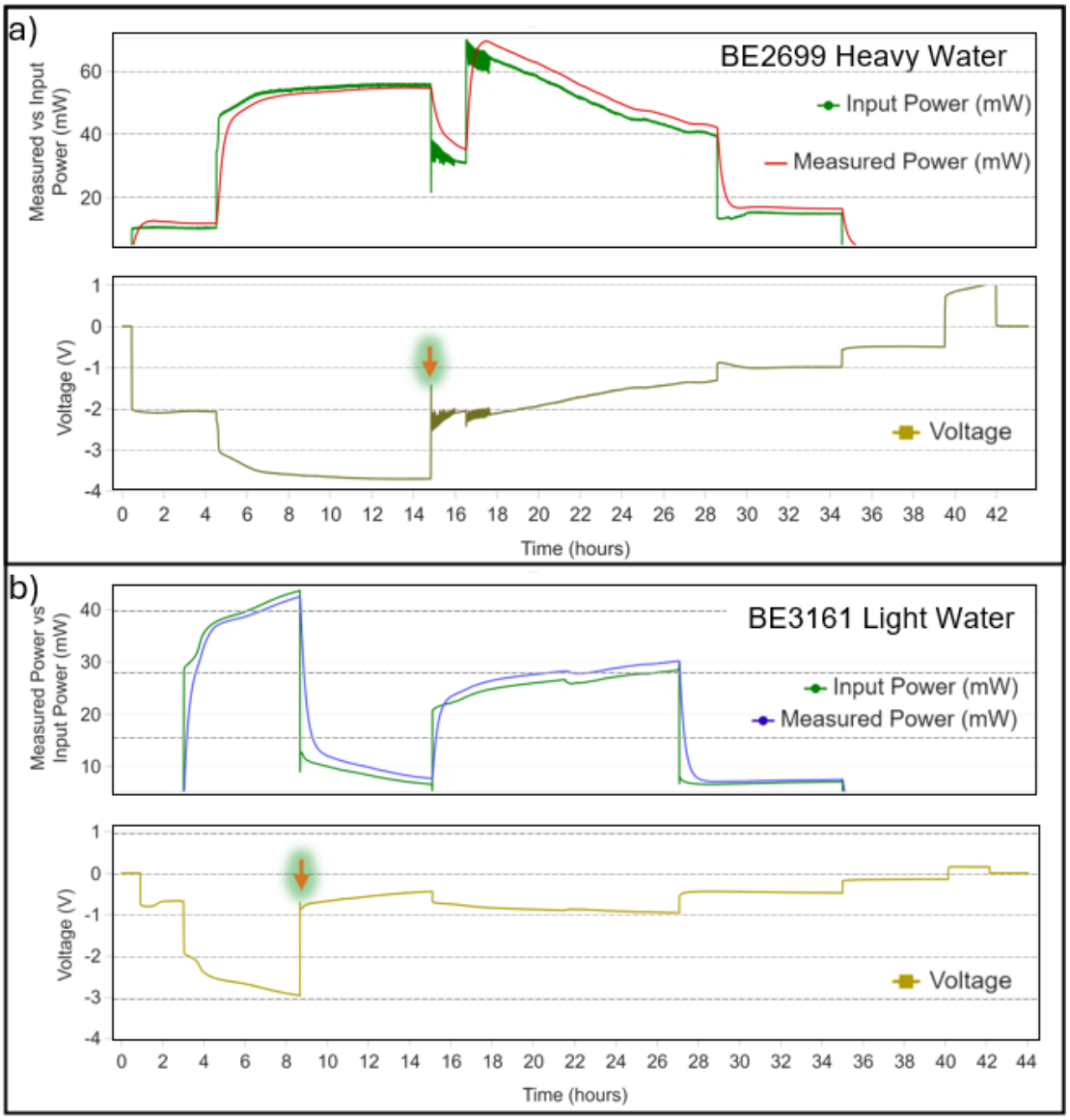

Figure 18: a) Heavy water HPE experiment showing a voltage instability form between 14-15 hours after which measured power remains above the calculated input power. b) Same results but in Light water and with only Pt electrodes.

Conclusion

While maintaining exceptional thermal and electrical isolation of the differential calorimeter channels, the parameter space explored in these calorimeter studies has not produced any definitive signal of LENR based AHE phenomena. Through passive calorimetry experiments probing set temperatures from -150-200 °C at gas pressures up to 150 ksi, spontaneous lattice enhanced D-D fusion (i.e., using unstimulated PdD) could not be detected through the bulk direct heat flow detection mechanism used in calorimetry. Stimulated Pd samples, regardless of sample form factor were heated up to 350 °C in near unity loading conditions with no excess heat measured by any of the Setaram calorimeters employed. Under any of the experimental conditions completed during this campaign, no environment was produced in either equilibrium or highly transient states that delivered quantifiable levels of AHE.

Calorimetry Appendix

This decision to directly interpret the voltage potential read out was made for the following reasons. Firstly, the system was a closed-type calorimeter with no additional energy or mass inputs once the channels were isolated at 100 or 150 ksi pressure with ultrapressure valves located on the outside of the calorimeter. As stated in the concept section the absence of additional inputs to the system we are monitoring minimizes the noise measured by each thermopile, maximizing the signal to noise ratio for actual sample-based reactions or perturbations. The raw potential signal, based off a known, stable baseline signal, can be interpreted directly to indicate if either channel's heat flux, control or active, is increasing or decreasing over time. Secondly, converting the potential signal to power using the thermal calibration coefficient [68]only provides a scaling factor to the already existing profile in the heat flux (μV) data since we used constants based on linear calibrations. The conversion to power becomes truly important when we do see a signal and we want to understand how much energy over time was released or absorbed into one of the sample channels.

[68] Thermal calibration coefficient (*K):* ($\mu V.mW^{-1}$) is used to convert electrical signal from the heat flux sensors (thermopiles) to the differential power inside the system. This study used a liner coefficient which was sufficient to assume the calibration as linear across the full range of the thermopile (-20000 to 20000 μV).

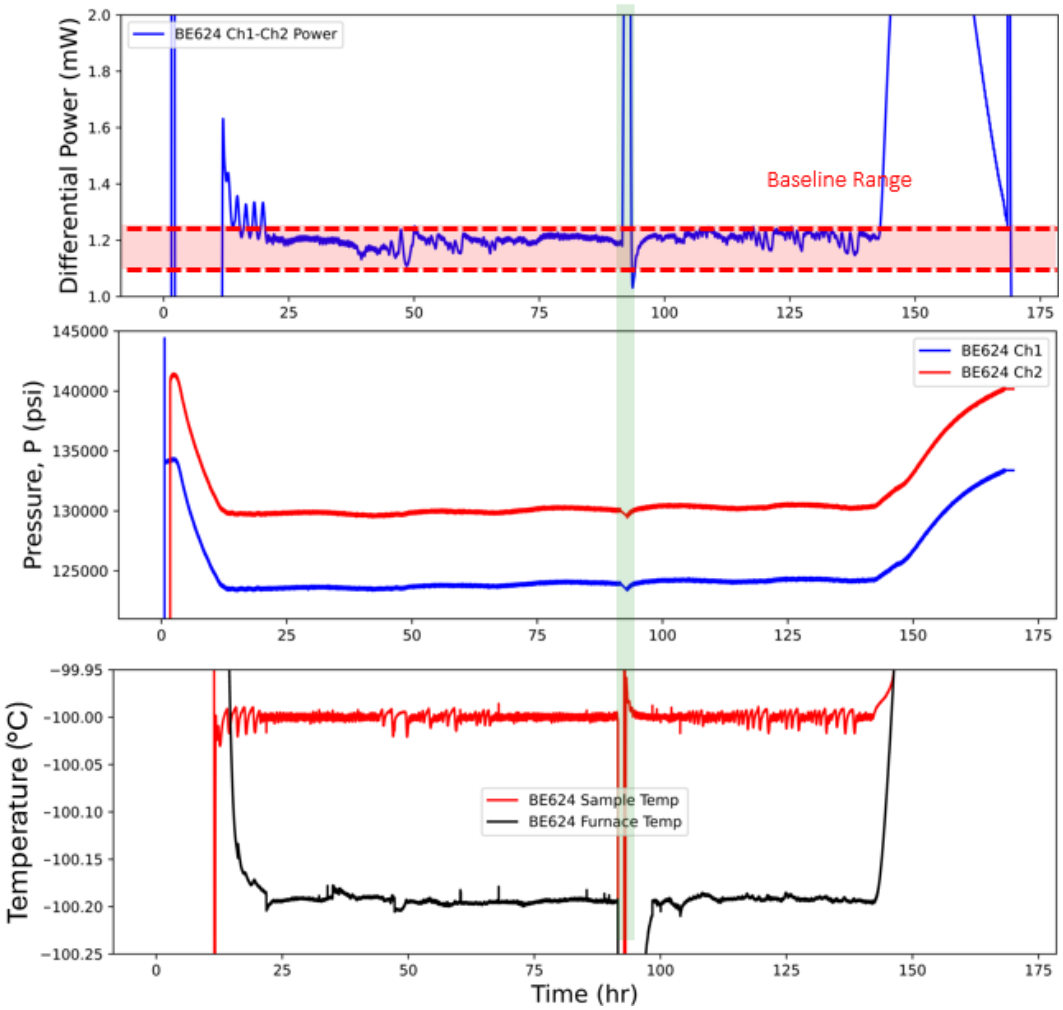

Figure 19: Heat flow results from another cryo-calorimtery test at 130 ksi in both H and D gases. Pressure decreases during cooling, explaining the drop from 140 to 130 ksi. At 90 hours the calorimeter heater shut off leading to a temperature dip to -150 °C, this was caught and corrected within 5 hours of the event. Sensitivity in this passive test was <0.5 mW.

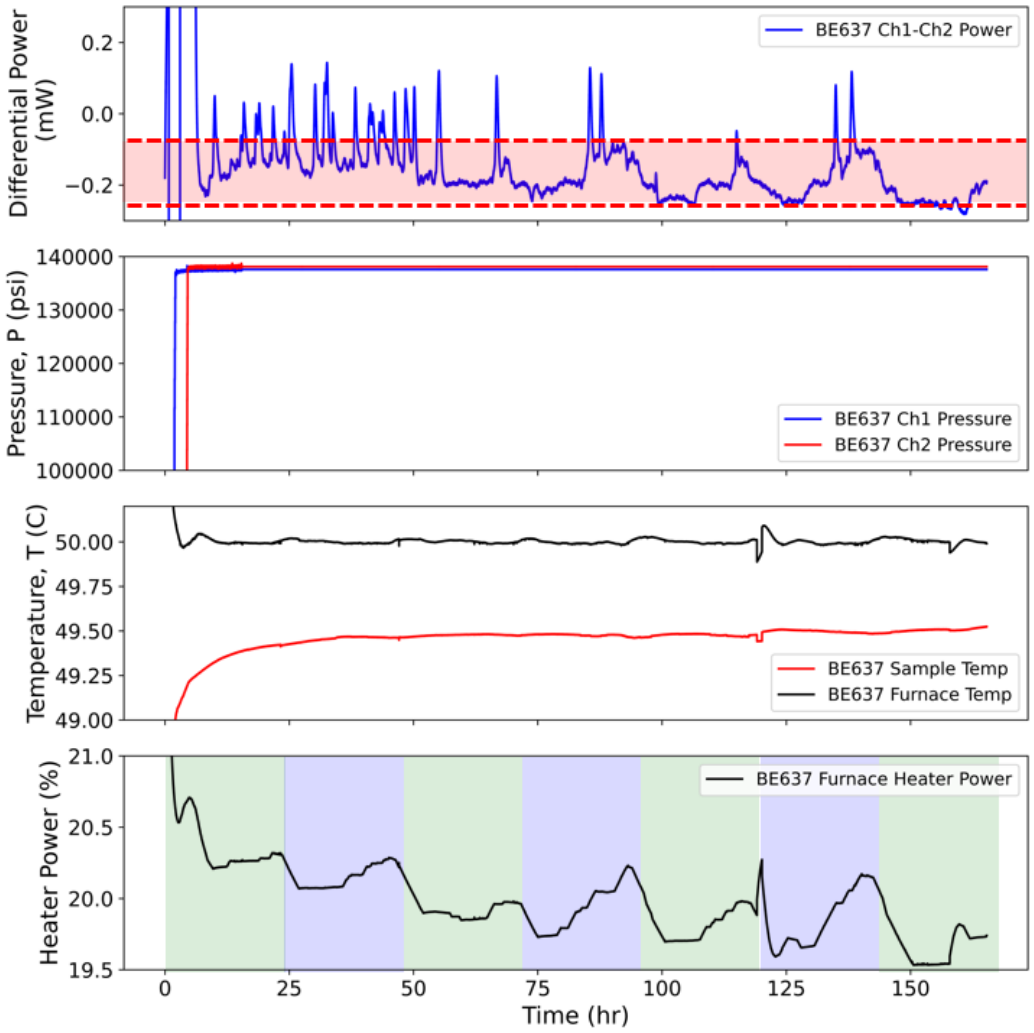

Figure 20: Auxiliary data included for BE637 that showed these odd heat spike events. Pressure and temperature trends show nothing correlating with these spikes. The heater power from the calorimeter itself is slowly decreasing over time and showing cyclical behavior over 24 hours due to small fluctuations in the temperature of the room the calorimeter enclosure was in. Blue and green zones designate 24 hour increments for the eye to follow easily.

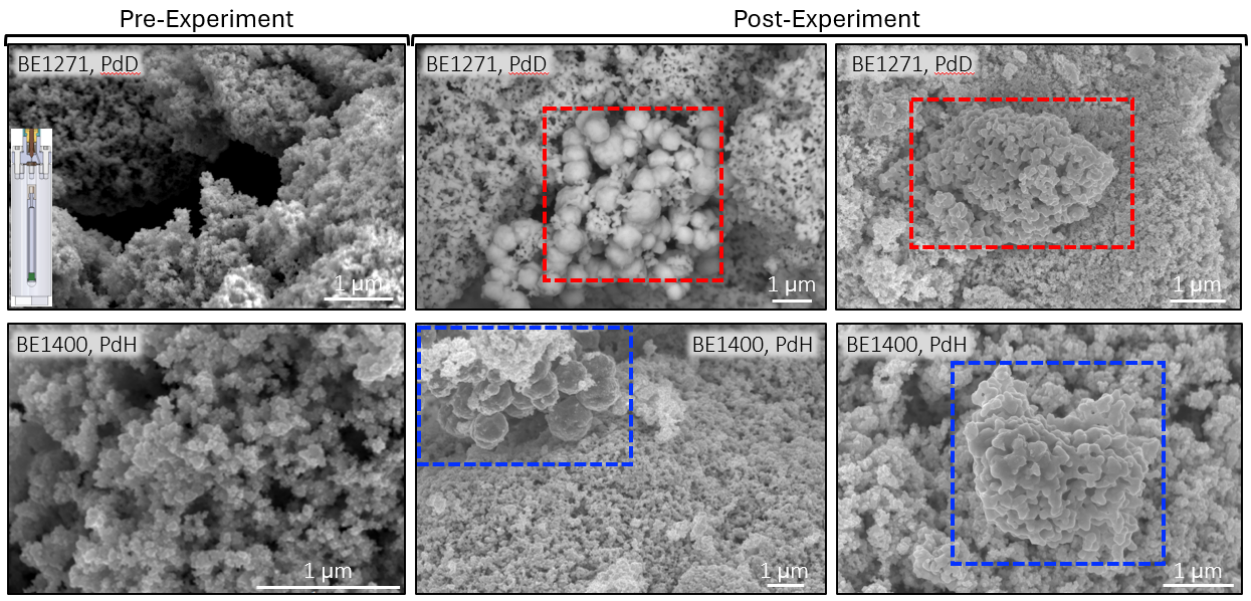

Figure 21: Pre and post SEM images of nanopowder used in passive calorimetry experiments for both protium and deuterium. Agglomerations of nanoparticles can be seen in post images independent of the gas isotope. We were also able to produce these agglomerations from pressurizing alone with nitrogen indicating this is a possible mechanical compression effect or these agglomerations always existed and were not caught in pre imaging procedures.

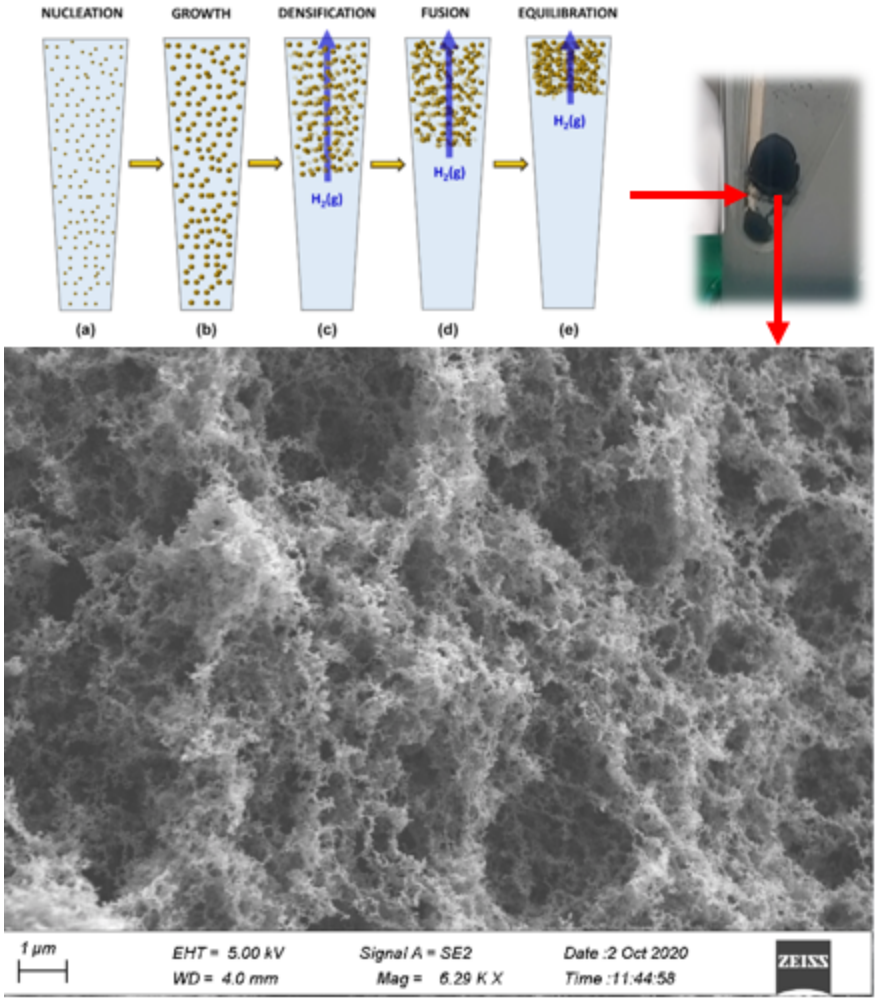

Figure 22: Simplified diagram of the process of how the aerogel and nanopowders were made inhouse and through external vendor. The nucleation rate, Growth, and densification were controlled through initial molarity, solvent temperature, and reaction time to obtain reproducible results. These fused nanostructures dehydrated from their solvent through sublimation freeze drying in high vacuum conditions over 24 hours. (Note: We could not confirm external vendor processing protocol but based off identifiable elemental contamination found in the vendors product we are confident they utilized the same precursor salts and solvents to obtain these nanostructures.)

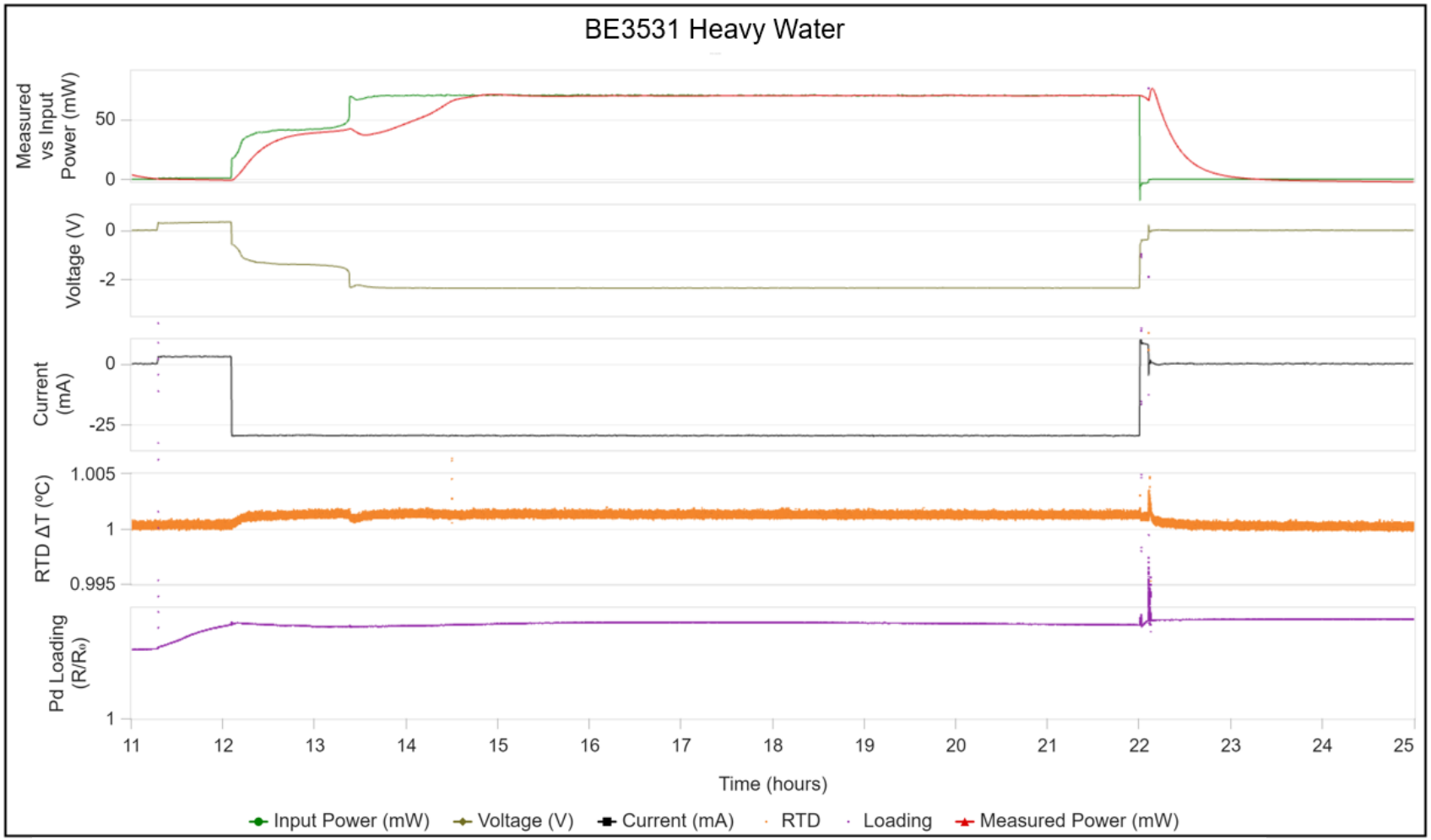

Figure 23: Auxiliary data for HPE calorimetry test in heavy water. Here we are showing how loading (R/R0), solvent temperature, and measured power change over time due to changes in voltage, current and voltage on the electrochemical circuit.

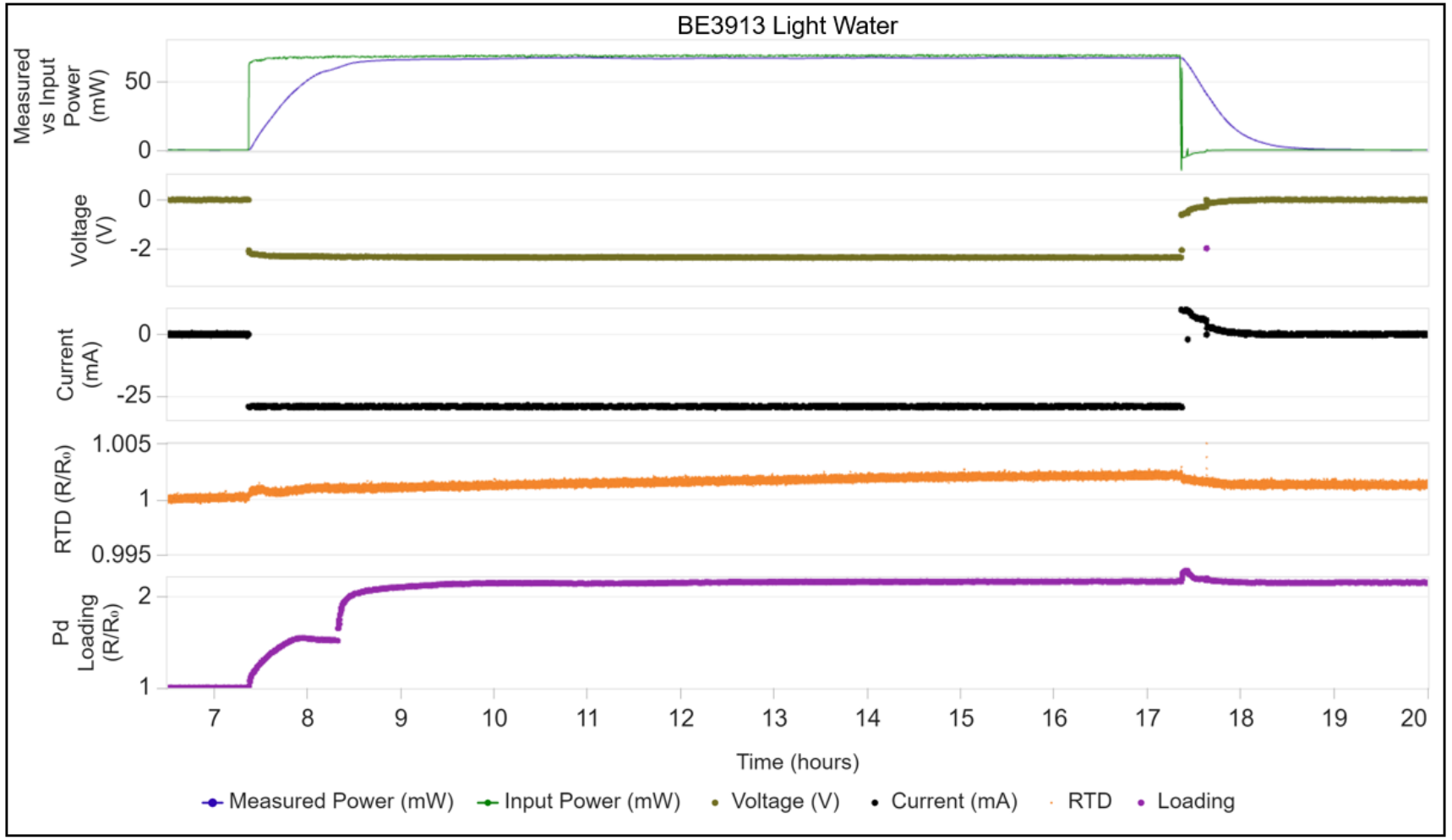

Figure 24:Auxiliary data for HPE calorimetry test in light water. Here we are showing how loading (R/R0), solvent temperature, and measured power change over time due to changes in voltage, current and voltage on the electrochemical circuit.

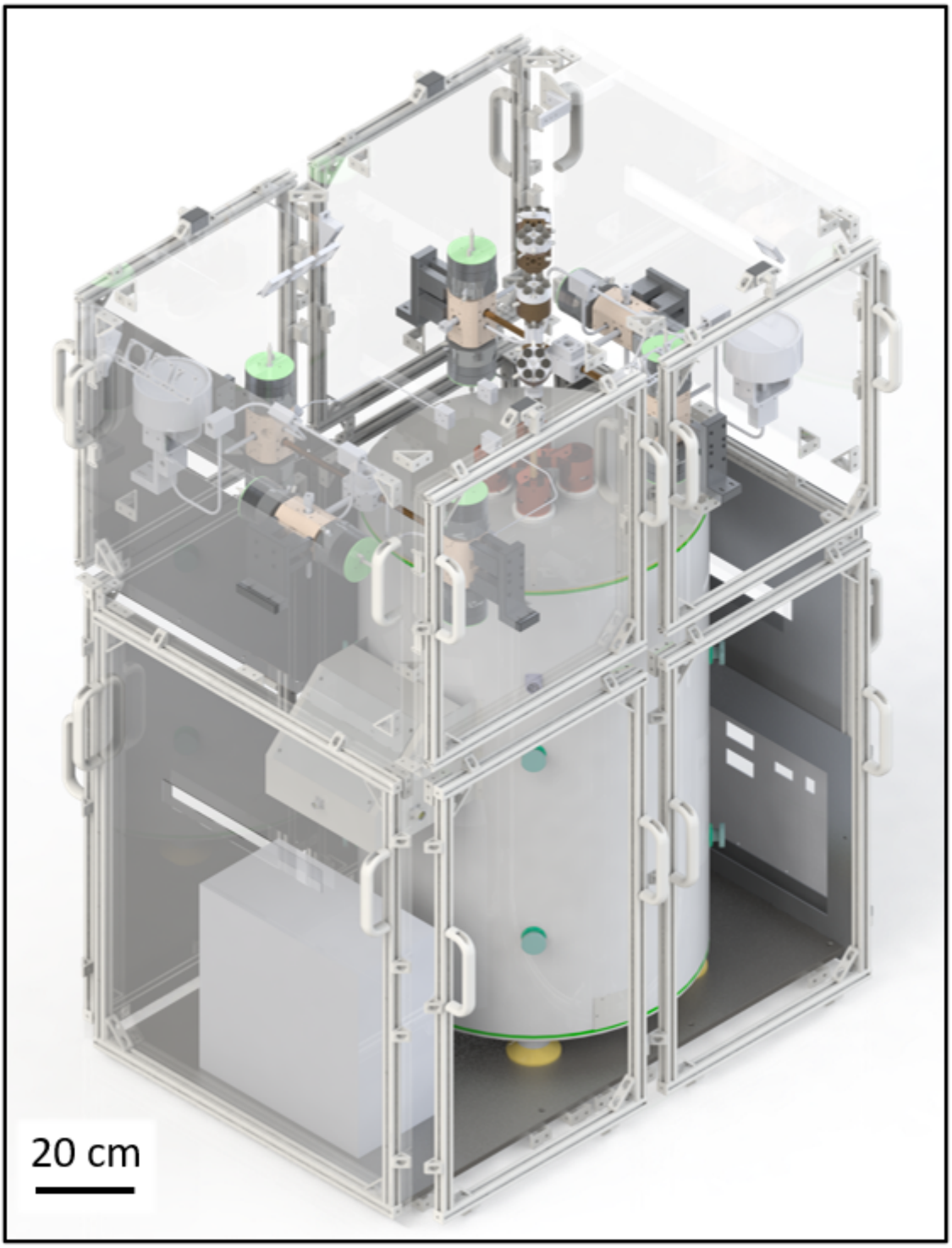

Figure 25: MS80 Thermal Enclosure, isometric view. The cart includes the MS80 calorimeter, 12 ultrapressure gas valves, and temperature and humidity PID controls to always maintain a constant 30 +/- 0.5 °C around the calorimeter shell.